Journal of Power Sources 214 (2012) 185–194

Contents lists available at SciVerse ScienceDirect

Journal of Power Sources

journal homepage: www.elsevier.com/locate/jpowsour

Carbon tolerance, electrochemical performance and stability of solid oxide fuel cells with Ni/yttria stabilized zirconia anodes impregnated with Sn and operated with methane

Anand Singh, Josephine M. Hill*

Department of Chemical and Petroleum Engineering, Schulich School of Engineering, 2500 University Dr. N.W., University of Calgary, Calgary, Alberta T2N 1N4, Canada

HIGHLIGHTS

- The addition of Sn did not improve the carbon tolerance of Ni/YSZ anodes in CH_4.
- The electrochemical performance decreased with Sn content.
- High amounts of Sn (5%) may impede the carbon removal reactions.
- The stability in CH_4 was similar for the Ni/YSZ and Sn-impregnated Ni/YSZ anodes.
- Sn content in the anode decreased after operation at 1073 K for 30 h.

ARTICLE INFO

Article history:
Received 12 March 2012
Received in revised form
18 April 2012
Accepted 20 April 2012
Available online 27 April 2012

Keywords:
Solid oxide fuel cell
Ni/YSZ anode
Sn-impregnated Ni/YSZ anode
Carbon deposition
Direct methane utilization
Electrolyte-supported cell

ABSTRACT

Carbon formation on conventional Ni/YSZ anodes is a major problem when solid oxide fuel cells (SOFC) are operated with hydrocarbons. Carbon formation reduces the operational stability and lifetime of SOFC. In this paper, the influence of the addition of Sn to Ni/YSZ anodes (100 micron) on the carbon tolerance, electrochemical performance and stability of the anodes when operated with CH_4 is studied. Sn is incorporated into the Ni/YSZ anodes of electrolyte-supported SOFC by impregnation (1 and 5 wt% Sn with respect to Ni). Addition of Sn to Ni/YSZ anodes does not reduce the carbon formation when SOFC are operated with CH_4 at low steam to carbon ratios (<0.03) and high temperatures (1013 and 1073 K). Severe coking and metal dusting occurs on Sn-impregnated Ni/YSZ anodes when operated at OCV and 1073 K with dry CH_4. Addition of higher amounts of Sn (5%) reduces electrochemical performance of Ni/YSZ anodes in H_2 and also reduces the carbon gasification rates, leading to higher carbon accumulation. The Sn content in the anode decreases after operation at 1073 K for 30 h. Hence retaining Sn in the anode might be difficult in actual stack operations at high temperatures (1073 K) and long durations ($>40{,}000$ h).

1. Introduction

Solid oxide fuel cells (SOFC) convert the chemical energy of fuels into electrical energy. The main applications of SOFC are for stationary power generation units and auxiliary power units in the transportation sector [1]. SOFC are operated at high temperatures (773–1273 K) [1,2] to overcome the high energy barriers associated with oxygen dissociation at the cathode and oxide ion diffusion through the solid oxide electrolyte, typically yttria stabilized zirconia (YSZ). The high temperature operation enhances reaction kinetics and permits the use of non-noble metals, such as Ni, as electrochemical oxidation catalysts in the anode. SOFC have several advantages including high efficiency, fuel flexibility and generation of high quality waste heat. The high quality waste heat can be used in cogeneration units to generate steam for space heating, industrial processing, or for more electricity generation in a steam turbine.

Presently, H_2 is the fuel of choice for fuel cells. However, 96% of H_2 is produced from hydrocarbons [3] and hence it may make more sense to use hydrocarbons directly as fuel [4]. Direct utilization of hydrocarbons like CH_4 in an SOFC, without a pre-reforming step to generate H_2 or syngas, would simplify and improve the overall efficiency of the system [3]. Ni is an excellent electrocatalyst but it also catalyzes the decomposition of hydrocarbons and formation of carbon. The primary carbon formation reaction is the Ni catalyzed decomposition of CH_4 via dissociative adsorption (reactions (1) and (2)) [5].

* Corresponding author. Tel.: +1 403 210 9488; fax: +1 403 284 4852.
E-mail address: jhill@ucalgary.ca (J.M. Hill).

0378-7753/$ – see front matter © 2012 Elsevier B.V. All rights reserved.
doi:10.1016/j.jpowsour.2012.04.062

$$CH_4 + * \leftrightarrow CH_x - * + \frac{(4-x)}{2}H_2 \quad (1)$$

$$CH_x - * \leftrightarrow C - * + \frac{x}{2}H_2 \quad (2)$$

Hydrogen and carbon produced from reactions (1) and (2) can be electrochemically oxidized as shown in reactions (3) and (4). The carbon can also react with water (reaction (5)) produced electrochemically at the anode or supplied with the fuel.

$$H_2 + O^{2-} \leftrightarrow H_2O + 2e^- \quad (3)$$

$$C + O^{2-} \leftrightarrow CO + 2e^- \quad (4)$$

$$C + H_2O \leftrightarrow CO + H_2 \quad (5)$$

At lower temperatures, typically below 973 K, the carbon monoxide produced can undergo disproportionation (reaction (6), Boudouard reaction) to produce carbon.

$$2CO \leftrightarrow C + CO_2 \quad (6)$$

Among the above reactions possible at the anode, reactions (1), (2), (6) and reverse of reaction (5) are carbon forming reactions and reactions (4), (5) and reverse of reaction (6) are carbon removal reactions. When the rate of carbon forming reactions exceeds the rate of carbon removal reactions, accumulation of carbon occurs. The accumulation of carbon can block the pores and result in expansion of the anode [6], causing damage to the SOFC.

To avoid carbon formation, higher steam: carbon ratios have been used [7], and non-coking materials including Cu/CeO_2/YSZ [3,8,9], $La_{0.75}Sr_{0.25}Cr_{0.5}Mn_{0.5}O_3$ (LSCM) [10], $La_{4.0}Sr_{8.0}Ti_{11.0}Mn_{0.5}Ga_{0.5}O_{37.5}$ (LSTMG) [11] and Sr_2MgMoO_6 (SMMO) [12] have been introduced to the anodes. Anodes made from these oxides have comparable anodic polarization resistances with Ni/YSZ anodes but have lower electrical conductivities. In reducing anode atmospheres, LSCM, LSTMG and SMMO had conductivities of 1.7 S cm^{-1} [13], 0.5 S cm^{-1} [11] and 10 S cm^{-1}[12], respectively, compared to >300 S cm^{-1} for Ni/YSZ anodes [14,15]. The low lateral conductivity (or high sheet resistance) of the above perovskites may result in low power densities, especially for SOFC designs with long current collection paths, as in fuel cell stacks [16] and also in tubular designs [10,17].

Ni/YSZ anodes have good electrochemical activity, high conductivity, ease of fabrication, thermal and chemical compatibility with electrolyte (YSZ). Due to these desirable properties, efforts have been made to improve the carbon tolerance of Ni/YSZ anodes by the addition alkaline earth oxides, such as CaO [18,19] and BaO [20] or by doping with metals such as Ru, Pd, Pt [21], Au [22,23], Ag [24] and Sn [25–27]. As addition of these precious metals to Ni is not economically viable, lower cost metals such as Sn, which has been shown to reduce carbon formation for steam reforming processes [5], have also been investigated. Recent studies [25–27] report that 1% Sn-doped Ni/YSZ thick (>1000 μm) anodes have superior operational stability in CH_4 than Ni/YSZ anodes. The role of Sn in reducing the carbon formation is attributed to Sn displacing Ni [28] from the carbon nucleation centers (defect step sites [29]) on the Ni catalyst, which lowers the binding energy of carbon on these sites, thereby reducing the nucleation of carbon [28].

Previous studies with Sn-doped Ni/YSZ anodes have been done with anode-supported SOFC with anode thicknesses of 1000 μm [25] and 1200 μm [26,27]. The present study is part of a project to develop planar metal-supported SOFC, which have thin anodes in the range of 10–100 μm. Thus, in this study thin (~100 μm thick) Ni/YSZ anodes with and without Sn and supported on thick electrolytes (~600 μm) have been fabricated and their performance compared. The prepared anodes were characterized with scanning electron microscopy (SEM), energy-dispersive X-ray spectroscopy (EDX), X-ray photoelectron spectroscopy (XPS), linear sweep voltammetry (*i*–*V*) and electrochemical impedance spectroscopy (EIS). The cells were tested in H_2 and CH_4 at 1013 K and 1073 K.

2. Experimental

Electrolyte-supported cells with ~100 μm thick anodes were used for this study. The anode powder was prepared by mixing NiO (50.6 wt%, Alfa Aesar, USA) with YSZ (43.1 wt%, TZ-8Y; Tosoh Co, Japan) and graphite (6.3 wt%, Alfa Aesar, USA) by ball milling in acetone for 24 h. The powders were dried and sieved to particle sizes less than 150 μm. The anode powder was then mixed with glycerol to make a slurry suitable for brush painting. Electrolytes were fabricated by uniaxially die pressing YSZ powder to a pressure of 53 MPa and then sintering at 1723 K for 2 h. The anode slurry was brush painted on the electrolyte and sintered at 1723 K for 2 h. The cathode powder was prepared by mixing $La_{0.8}Sr_{0.2}MnO_3$ (40 wt%, LSM, Praxair Specialty Ceramics, USA) with YSZ (40 wt%) and graphite (20 wt%). The cathode powder was mixed with glycerol and applied on the other side of the electrolyte and sintered at 1523 K for 2 h. The thickness of the cathode (LSM/YSZ) and electrolyte (YSZ) were 80 and 600 μm, respectively. Sn was incorporated into the porous, sintered NiO/YSZ anode-substrate by impregnating a solution of $SnCl_2 \cdot 2H_2O$ (Aldrich, USA) dissolved in ethanol, followed by calcination at 773 K for 4 h. The target Sn loadings were 1 and 5 wt% with respect to Ni. The Ni/YSZ anodes impregnated with 1 and 5% Sn were labeled as 1% SnI–Ni/YSZ and 5% SnI–Ni/YSZ, respectively (where I refers to impregnated). The area of the anode and cathode was 0.9 cm^2. The anode side of the cell was attached to an alumina tube using ceramic paste (552 VFG, Aremco, USA). A quartz tube was used to supply the fuel gas into the anode side and the cathode was exposed to air.

SOFC with Ni/YSZ, 1% SnI–Ni/YSZ and 5% SnI–Ni/YSZ anodes were tested at 1013 and 1073 K. The flow rate of humidified and dry H_2 was 50 ml min^{-1}, while that of humidified and dry CH_4 was 25 ml min^{-1}. The current collectors on the anode and cathode sides were Ag wire loops (Alfa Aesar, USA) attached to the electrodes using Ag paste (Alfa Aesar, USA). Electrochemical measurements were done using an electrochemical interface (1287 Potentiostat and 1260 Frequency response analyzer, Solartron Analytical, U.K.). The cells were characterized by *i*–*V*, galvanostatic, potentiostatic and EIS measurements. Impedance spectra were measured at equilibrium (OCV) with AC amplitude of 10 mV in the frequency range of 0.1 Hz–1 MHz. In some cases impedance spectra were measured at 10 mA cm^{-2} with amplitude of 1 mA in the same frequency range. All the cells were initially tested in dry and humidified H_2 at the operating temperatures. During these initial tests with H_2; the quality of the sealing, stability and performance of the cells in dry and humidified H_2 were analyzed. Once stable performance was achieved with H_2, the cells were tested with CH_4. The cell test protocol was kept constant for all cells with Ni/YSZ, 1% SnI–Ni/YSZ and 5% SnI–Ni/YSZ anodes, for the different operating conditions.

The carbon formed on the anodes was analyzed by temperature programmed oxidation (TPO) and SEM (Philips ESEM-XL30). For TPO measurements, the tested cell was exposed to 10% O_2/bal He gas at a flow rate of 50 ml min^{-1}. The sample was heated from room temperature to 1173 K at the rate of 10 K min^{-1}. The exhaust gases were analyzed using a mass spectrometer (Cirrus 200 Quadrupole,

MKS, USA). The Sn content in the anodes was analyzed by EDX and XPS.

3. Results and discussion

3.1. Electrochemical performance in H_2

The electrochemical performance of SnI–Ni/YSZ anodes was compared with that of Ni/YSZ anodes in dry and humidified H_2. These experiments were done in order to understand the influence of Sn addition on the electrochemical performance of Ni/YSZ anodes. Fig. 1a and b show i–V curves of the best performing cells containing Ni/YSZ, 1% SnI–Ni/YSZ or 5% SnI–Ni/YSZ anodes in dry and humidified H_2, respectively, at 1073 K. Fig. 1c shows the electrochemical impedance spectra of the same cells in humidified H_2 at OCV and 1073 K. Six cells with each type of anode (18 cells total) were tested and the average maximum power densities for SOFC with Ni/YSZ, 1% SnI–Ni/YSZ and 5% SnI–Ni/YSZ anodes were 83 ± 7, 83 ± 12, and 61 ± 8 mW cm^{-2}, respectively, in dry H_2, and 81 ± 6, 78 ± 14, and 59 ± 7 mW cm^{-2}, respectively, in humidified H_2 (Fig. 2). The average polarization resistances of SOFC with Ni/YSZ, 1% SnI–Ni/YSZ and 5% SnI–Ni/YSZ were 2.8, 3.6 and 5.1 Ω cm^2, respectively, in humidified H_2 (note, the best performing cells are shown in Fig. 1a–c). The electrochemical performance was similar for SOFC with Ni/YSZ and 1% SnI–Ni/YSZ anodes. The power density decreased significantly for the SOFC with 5% SnI–Ni/YSZ anodes. This decrease in performance corresponded to an increase in polarization resistance (Fig. 1c). SOFC tested at a lower temperature of 1013 K, similar to testing conditions used by Nikolla et al. [25], also showed a decrease in electrochemical performance as the Sn content in the Ni/YSZ anode was increased (Fig. 3). Similar decreases in electrochemical performance with Sn content have been observed previously [25,26,30].

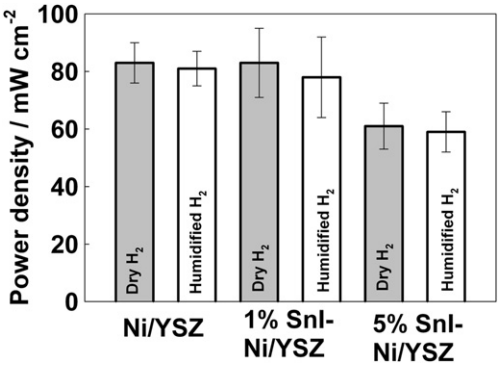

Fig. 2. Average maximum power density of six SOFC with Ni/YSZ, 1% SnI–Ni/YSZ and 5% SnI–Ni/YSZ anodes in dry and humidified H_2 at 1073 K.

Nikolla et al. [25] attributed this decrease in performance to the formation of a separate Sn oxide phase which would decrease the electronic conductivity of the anode. A decrease in electronic conductivity on adding Sn was not observed in this study. The ohmic resistance at 1013 K of SOFC with Ni/YSZ, 1% SnI–Ni/YSZ and 5% SnI–Ni/YSZ were 2.21, 2.21 and 2.17 Ω cm^2, respectively. The average ohmic resistance at 1073 K of six SOFC with Ni/YSZ, 1% SnI–Ni/YSZ and 5% SnI–Ni/YSZ were 1.6 ± 0.08, 1.5 ± 0.06 and 1.5 ± 0.07 Ω cm^2, respectively. There was, however, an increase in the polarization resistance with the addition of Sn as shown in Fig. 1c. The observed decrease in performance may be attributed to the increase in polarization resistance on adding Sn. XPS analysis of a reduced 2% SnI–Ni/YSZ anode, prepared in the preliminary phase of this work, indicated a Sn/Ni weight ratio of 22% showing that most of the Sn in the Ni particle was concentrated at the surface of the particle. This high concentration of Sn at the Ni surface may lead to Sn occupying the electrochemically active Ni sites [26,30] thereby increasing the polarization resistance.

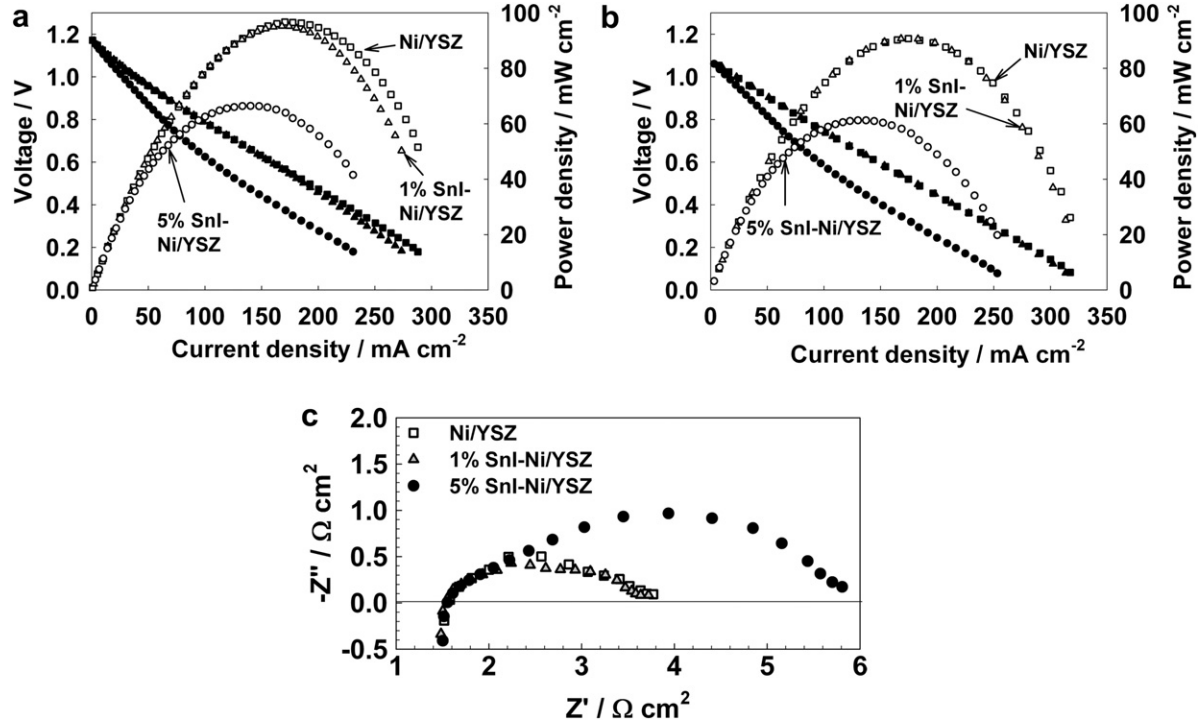

Fig. 1. Power density (open symbols) and cell voltage (filled symbols) as a function of current density for SOFC with Ni/YSZ (□, ■), 1% SnI–Ni/YSZ (Δ, ▲) and 5% SnI–Ni/YSZ (○, ●) anodes at 1073 K in (a) dry H_2, (b) humidified H_2 and (c) electrochemical impedance spectra of the same cells in humidified H_2 at OCV and at 1073 K.

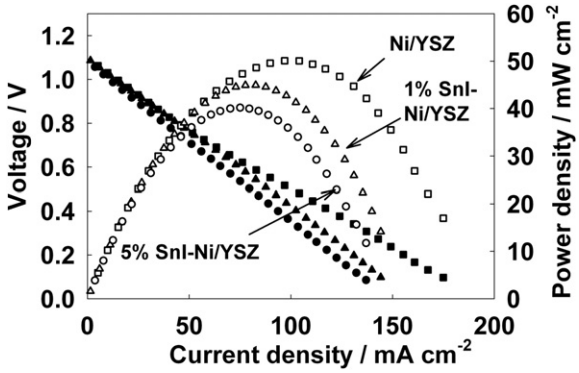

Fig. 3. Power density (open symbols) and cell voltage (filled symbols) as a function of current density for SOFC with Ni/YSZ (□, ■), 1% SnI–Ni/YSZ (Δ, ▲) and 5% SnI–Ni/YSZ (○, ●) anodes at 1013 K in humidified H_2.

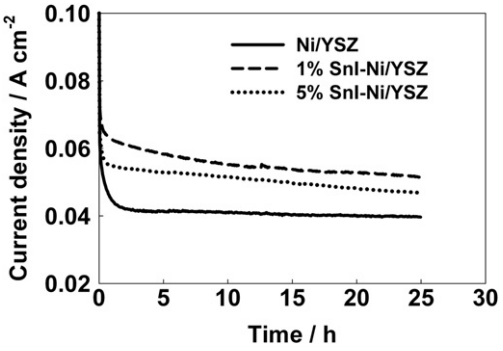

Fig. 5. Current density as a function of time for SOFC with Ni/YSZ (solid line), 1% SnI–Ni/YSZ (broken line) and 5% SnI–Ni/YSZ (dotted line) anodes operated at 0.6 V in dry CH_4 at 1013 K for 25 h.

3.2. Electrochemical performance and operational stability in CH_4

The electrochemical performance and operational stability of the SOFC were tested at 10 mA cm^{-2} in dry CH_4 (Fig. 4a) and 50 mA cm^{-2} in humidified CH_4 (Fig. 4b) at 1073 K. Also SOFC were tested at 1013 K in dry CH_4 at 0.6 V (Fig. 5) similar to testing conditions studied by Nikolla et al. [25]. The degradation rates over the last 10 h (15–25 h of operation) of the galvanostatic and potentiostatic tests (Figs. 4 and 5) are reported in Table 1. During operation at 10 mA cm^{-2} at 1073 K (Fig. 4a) and 0.6 V at 1013 K (Fig. 5) in dry CH_4, the SOFC with Ni/YSZ anodes had slightly lower performance and also lower degradation rates than those with SnI–Ni/YSZ anodes. During operation at 50 mA cm^{-2} in humidified CH_4 at 1073 K (Fig. 4b), the SOFC with a Ni/YSZ anode initially had a lower operating voltage, but steadily increased to a higher operating voltage than those with SnI–Ni/YSZ anodes. The differences in carbon formation, electrochemical and non-electrochemical reaction rates may be responsible for the observed performance differences between the Ni/YSZ and SnI–Ni/YSZ anodes under different operating conditions. The electrochemical studies, however, do not isolate the chemical or structural changes responsible for the observed differences [31]. Recent advances in in-situ characterization techniques [31,32] may be able to better isolate the factors responsible. Increasing the Sn content from 1 to 5% decreased the electrochemical performance in all cases.

Nevertheless, no catastrophic decrease in performance was observed at the above three operating conditions, unlike those observed in previous studies [26,27] involving anode-supported SOFC. The difference in the cell design, namely electrolyte-supported in the present study versus anode-supported in the previous studies [26,27], may be responsible for this difference. Formation of carbon induces mechanical stress in the anode, and this stress will be greater for anode-supported cells than electrolyte-supported cells. The anode in an anode-supported cell is more constrained because it is sealed to the testing apparatus using ceramic or glass sealants and has inherent rigidity because of its thickness. In electrolyte-supported cells, the sealing is done between the electrolyte and the testing apparatus, which allows more expansion for the anode. In the above three operating conditions, there was no strong correlation between the accumulated carbon (Table 2) and the improvement or degradation in performance. Also no significant difference in the operational stability could be observed between the Ni/YSZ and SnI–Ni/YSZ anodes. The carbon formed at the above operating conditions in this study may not be sufficient to significantly affect the anode structure or the electrochemical performance, by either blocking the pores or affecting the electrochemical reaction.

The carbon formation rate can be accelerated by operating at OCV in dry CH_4 at 1073 K. Operation at OCV is a harsh operating condition for SOFC utilizing direct hydrocarbons as the highest amount of carbon will be formed under these conditions [33]. In real situations, SOFC may be operated at OCV or at conditions close to OCV during start-up and shut-down procedures, very low load, accidental load throw-off, etc. Normally these conditions are avoided during cell testing, or the cells are tested at OCV in direct hydrocarbon only for a very short time (long enough to record a steady OCV value), in order to avoid damaging the anode permanently before performing other electrochemical tests [34]. In this study, the cells were operated at OCV in dry CH_4 to better understand carbon formation on the anodes in the presence of Sn.

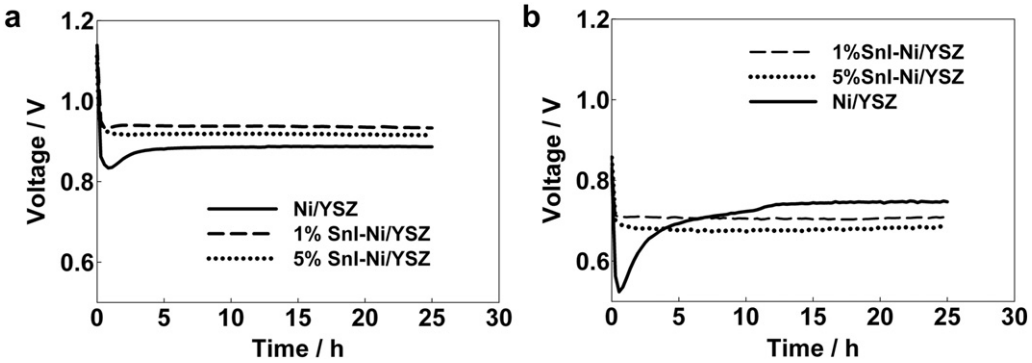

Fig. 4. Cell voltage as a function of time for SOFC with Ni/YSZ (solid line), 1% SnI–Ni/YSZ (broken line) and 5% SnI–Ni/YSZ (dotted line) anodes operated at 1073 K for 25 h in (a) dry CH_4 at 10 mA cm^{-2} and (b) humidified CH_4 at 50 mA cm^{-2}.

Table 1
Rate of change of power density of SOFC with Ni/YSZ, 1% SnI–Ni/YSZ and 5% SnI–Ni/YSZ anodes over a period of 10 h from the 15th to 25th h of operation in CH_4.

Anode	Dry CH_4; 10 mA cm^{-2}; 1073 K ($\mu W\ h^{-1}$)	Humidified CH_4; 50 mA cm^{-2}; 1073 K ($\mu W\ h^{-1}$)	Dry CH_4; 0.6 V; 1013 K ($\mu W\ h^{-1}$)
Ni/YSZ	−1.3	+16.5	−35.4
1% SnI–Ni/YSZ	−3.2	+19.5	−132
5% SnI–Ni/YSZ	−2.7	+34.5	−174

i–V curves were measured 1 h (Fig. 6a) and 25 h (Fig. 6b) after exposure to dry CH_4 under OCV conditions at 1073 K. SOFC with Ni/YSZ, 1% SnI–Ni/YSZ and 5% SnI–Ni/YSZ anodes had maximum power densities of 40, 47 and 36 mW cm^{-2}, respectively, after 1 h (Fig. 6a) and these values decreased to 35, 33 and 7 mW cm^{-2} after 25 h (Fig. 6b). The performance of all SOFC degraded (Ni/YSZ < 1% SnI–Ni/YSZ < 5% SnI–Ni/YSZ), with the severest degradation observed for the SOFC with the 5% SnI–Ni/YSZ anode. Fig. 7a and b shows the cross-sectional SEM images of Ni/YSZ and 5% SnI–Ni/YSZ anodes before electrochemical testing. After testing in dry CH_4 under OCV conditions at 1073 K, structural degradation of the anodes occurred with a significant size reduction of the anode particles (Fig. 7c and d). Such anode structural degradation was not observed when the SOFC were operated at 10 mA cm^{-2} in dry CH_4 (Fig. 7e and f) and 50 mA cm^{-2} in humidified CH_4, resulting in good operational stability (Fig. 4). Also, comparison of the SEM images in Fig. 7a,b and c,d shows that Sn does not induce any damage to the anode microstructure. The breakdown of the anode particles under OCV conditions (Fig. 7c and d) was likely caused by metal dusting in which graphite grows into the bulk nickel, disrupts its structure and converts it to dust [35]. Along with the Ni metal, metal dusting also caused the breakdown of the YSZ structural backbone and removal of material from the anode. This structural breakdown caused the reduction of the anode thickness from ~100 to ~25 μm (Fig. 8) after 25 h.

This degradation of the anode resulted in an increase in the ohmic resistances by 0.09, 0.32 and 10.14 Ω cm^2 for SOFC with Ni/YSZ, 1% SnI–Ni/YSZ and 5% SnI–Ni/YSZ anodes, respectively, after 25 h of operation in dry CH_4 under OCV conditions at 1073 K. The increase in ohmic resistance for the SOFC with 5% SnI–Ni/YSZ anodes was high because the metal dusting had affected the electrical contact between the Ag wire and the anode, whereas in the other two SOFC anodes the electrical contact had not been affected. The destruction of the anode microstructure also increased the polarization resistance. Fig. 9 shows the increase in ohmic and polarization resistance of the SOFC with 5% SnI–Ni/YSZ anode on exposure to dry CH_4 at OCV and 1073 K for 25 h. These increases in ohmic and polarization resistances were responsible for the performance degradation observed in Fig. 6. The degradation trend observed under OCV conditions in dry CH_4 (Ni/YSZ < 1% SnI–Ni/YSZ < 5% SnI–Ni/YSZ) was consistent with the amount of carbon formed on these anodes (Ni/YSZ < 1% SnI–Ni/YSZ < 5% SnI–Ni/YSZ) as shown in Table 2.

3.3. Carbon formation

The amount and type of carbon accumulated on an anode while utilizing direct hydrocarbons depends on the operating conditions including fuel conditions, temperature, current density, and anode thickness [33,36,37]. In this study, the influence of Sn addition to Ni/YSZ anodes on carbon formation at different operating conditions was studied. The SOFC were operated at (i) OCV, (ii) 10 mA cm^{-2} in dry CH_4, (iii) 50 mA cm^{-2} in humidified CH_4 at 1073 K and (iv) 0.6 V in dry CH_4 at 1013 K for 25 h. Thermodynamically all operating conditions were within the carbon formation region [36]. The OCV in dry H_2 at 1073 K was between 1.17 and 1.22 V for all the SOFC tested. These voltages correspond to an oxygen partial pressure of $1.93–0.22 \times 10^{-21}$ kPa in the anode, calculated using the Nernst equation for ambient pressure at Calgary, Canada (88 kPa). This low oxygen partial pressure shows that the quality of sealing was good and consistent. Good sealing is very important for carbon accumulation analysis as air leakage can influence the amount and type of carbon accumulated on the anode. The amount and type of carbon formed on the anodes of these SOFC were analyzed by TPO. Dedicated cell tests were performed for carbon formation analysis. In these cell tests, initial cell characterizations were done in dry and humidified H_2 and then cell operation was started in CH_4 at the conditions mentioned above for 25 h. During this operation in CH_4, no other electrochemical tests such as *i–V* or EIS were performed, as these tests influence the carbon accumulation results. After operation in CH_4, the cells were cooled down in He and analyzed by TPO.

During TPO analysis, the carbon accumulated on the anode is oxidized to produce CO_2 (Fig. 10), and if hydrogen is present with the carbon then H_2O will also be produced (Fig. 11). The amount of carbon or hydrogen is calculated from the area under the TPO peaks. A common feature in all the TPO profiles is the presence of CO_2 peaks and corresponding H_2O peaks between 500 and 800 K, indicating that the carbon that burns off between 500 and 800 K is associated with hydrogen as CH_x fragments. This carbon will be referred to as Type I carbon. The carbon that burns off between 800 and 1100 K is not associated with hydrogen and will be referred to as Type II carbon. The terminology Type I and Type II carbon are based on the terminology used by Finnerty et al. [38] and based on the temperature range at which the carbon reacts with oxygen during the TPO analysis.

The low burn-off temperature (500–800 K) of Type I carbon shows that it is weakly bonded to the Ni/YSZ [33]. In this temperature range, there are two CO_2 peaks (Inset of Fig. 10b, and Fig. 10c and d) for the cells tested under galvanostatic (10, 50 mA cm^{-2}) and potentiostatic (0.6 V) conditions. Our group [33] has previously reported multiple CO_2 peaks in the 500–825 K range for SOFC operated at 1, 10 and 50 mA cm^{-2} in dry CH_4 at 1073 K for 6 h. The carbon that burns off between 500 and 650 K has a H:C ratio of 2.8 ± 0.4 and between 650 and 800 K has a H:C ratio of 1.1 ± 0.2. The operating conditions or the presence of Sn did not significantly influence the amount of Type I carbon. When the anode is exposed to CH_4, the dissociative adsorption (reactions (1) and (2)) of CH_4 to

Table 2
Amount of carbon formed on SOFC anodes operated for 25 h in CH_4 under different operating conditions.

Anode	Carbon formed (mol carbon mol Ni^{-1})											
	OCV; dry CH_4; 1073 K			10 mA cm^{-2}; dry CH_4; 1073 K			50 mA cm^{-2}; humidified CH_4; 1073 K			0.6 V; dry CH_4; 1013 K		
	Total	Type I (%)	Type II (%)	Total	Type I (%)	Type II (%)	Total	Type I (%)	Type II (%)	Total	Type I (%)	Type II (%)
Ni/YSZ	2.20	3.2	96.8	0.047	70.8	29.2	0.039	75.8	24.2	0.035	81.5	18.5
1% SnI–Ni/YSZ	3.87	3.9	96.1	0.326	12.8	87.2	0.062	81.9	18.1	0.043	54.7	45.3
5% SnI–Ni/YSZ	7.05	2.6	97.4	0.331	8.1	91.9	0.093	61.6	38.3	0.090	39.6	60.4

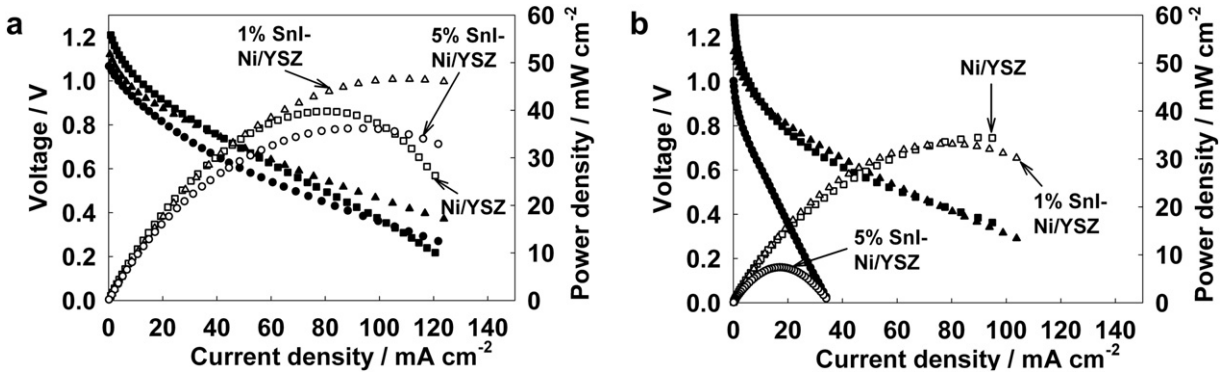

Fig. 6. Power density (open symbols) and cell voltage (filled symbols) as a function of current density for SOFC with Ni/YSZ (□, ■), 1% SnI–Ni/YSZ (Δ, ▲) and 5% SnI–Ni/YSZ (○, ●) anodes in dry CH_4 at 1073 K after operation at OCV condition for (a) 1 h and (b) 25 h.

CH_x fragments and monoatomic carbon occurs [5]. The amount of CH_x fragments or Type I carbon present in the anodes after testing in CH_4 appear not to be sensitive to the operating conditions or the type of anode. The amount of carbon in the 800–1100 K range (Type II) was, however, a strong function of the operating conditions. The results in Table 2 show that the relative quantity of Type II carbon decreased as the current density increased. The monoatomic carbon formed by the dissociative adsorption (Eqs. (1) and (2)) of CH_4 may be removed (reactions (4), (5) and reverse of reaction (6)) or polymerized to form less reactive carbon (Type II) [5]. The rates of these carbon forming and carbon removal reactions are dependent on the operating conditions and the anode. Type II carbon has been shown to be graphitic carbon by XRD analysis [27]. In other studies, the carbon deposited on a Ni/YSZ anode exposed to a feed of methane at 873 K [39] and 988 K [40] was observed to be graphitic by in-situ Raman spectroscopy analysis.

SnI–Ni/YSZ anodes had higher amounts of carbon than Ni/YSZ for all four operating conditions tested (Table 2). At OCV conditions, though dry CH_4 is used as fuel, there is a small partial pressure of oxygen ($1.93–0.22 \times 10^{-21}$ kPa) at the anode due to the leakage of air through the seals, which can remove some of the carbon. Because the oxygen partial pressure in the anode is small ($<10^{-21}$ kPa in all the SOFC tested), the carbon formation rate far exceeds the carbon removal rate, and carbon accumulation reflects the decomposition rate of CH_4. Under OCV conditions in dry CH_4, Sn does not appear to reduce the CH_4 decomposition rate.

Similarly, under other operating conditions, the higher the Sn content of the anode the more carbon was formed (Table 2). As the current density was increased, the oxygen content in the anode increased. In fact, at all operating conditions other than OCV, sufficient oxygen was supplied (4.17×10^{-3} mol at 10 mA cm^{-2}) over 25 h to remove all of the carbon that was formed (maximum of 2.35×10^{-3} mol at OCV in 25 h for the SOFC with 5% SnI–Ni/YSZ anode). The accumulation of carbon on Ni/YSZ and SnI–Ni/YSZ anodes indicates that not all the oxygen supplied participated in the carbon removal reactions (reactions (4), (5) and reverse of reaction (6)). The tests done at OCV in dry CH_4 at 1073 K showed that addition of Sn did not reduce the carbon formation. At the

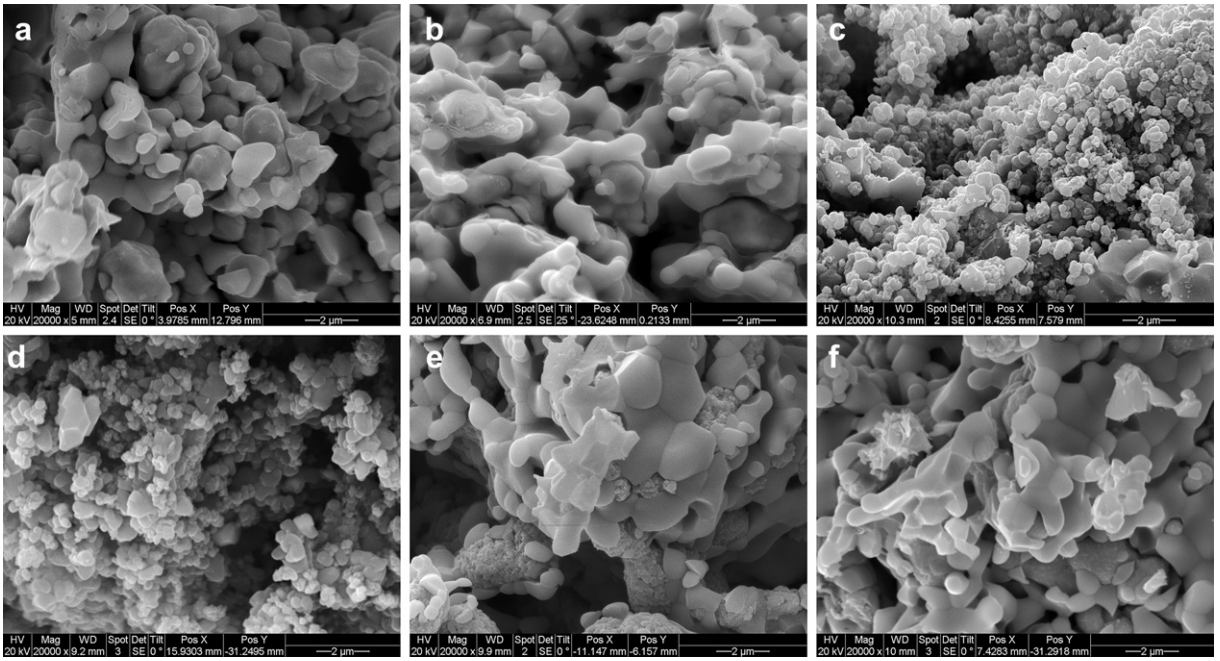

Fig. 7. SEM cross-sectional images of freshly prepared (a) Ni/YSZ anode and (b) 5% SnI–Ni/YSZ anode; (c) and (d) Ni/YSZ anode and 5% SnI–Ni/YSZ anodes, respectively, after operation at OCV and 1073 K in dry CH_4 for 25 h; (e) and (f) Ni/YSZ and 5% SnI–Ni/YSZ anodes, respectively, after operation at 10 mA cm^{-2} and 1073 K in dry CH_4 for 25 h.

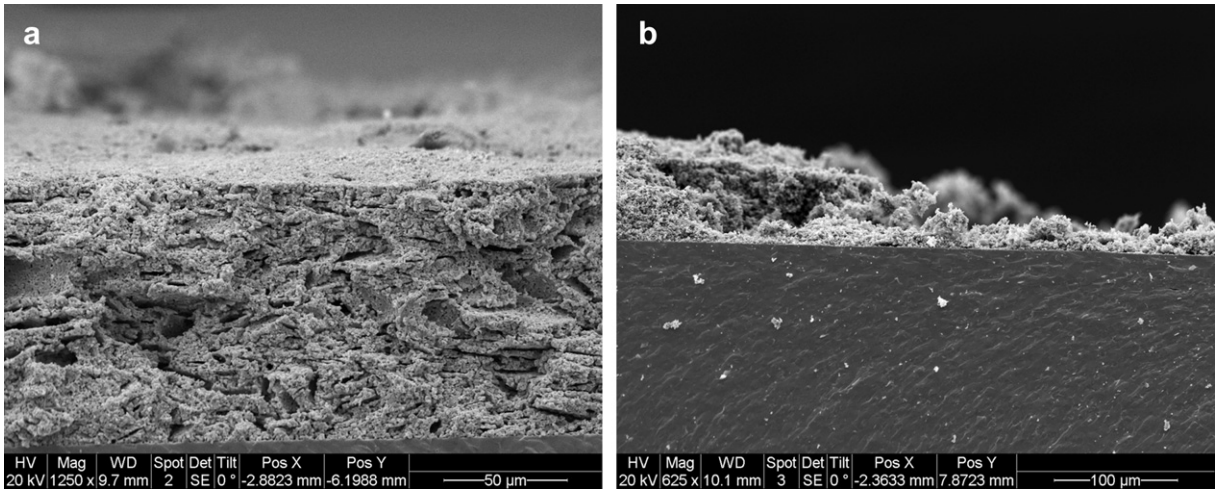

Fig. 8. SEM cross-sectional images of (a) freshly prepared Ni/YSZ anode, (b) Ni/YSZ anode after operation at OCV and 1073 K in dry CH_4 for 25 h showing reduction in anode thickness due to metal dusting.

other three operating conditions tested (10 mA cm^{-2} in dry CH_4, 50 mA cm^{-2} in humidified CH_4 and 0.6 V in dry CH_4), carbon removal reactions influenced the amount of carbon accumulated. At these conditions, it appears that the carbon removal reactions were more facile on the Ni/YSZ anodes than the SnI–Ni/YSZ anodes, and the presence of Sn may have impeded the removal of carbon on Ni.

Impedance analysis was done on the SOFC with Ni/YSZ and 5% SnI–Ni/YSZ anodes after operation at 10 mA cm^{-2} for 25 h at 1073 K in dry CH_4 to understand if there was any difference in the electrochemical reactions occurring at the anodes which would lead to higher carbon accumulation on the 5% SnI–Ni/YSZ anode. The impedance analysis was done at 10 mA cm^{-2} with amplitude of 1 mA in dry CH_4 at 1073 K. There was no difference in the polarization resistance between the SOFC with Ni/YSZ and 5% SnI–Ni/YSZ anodes (Fig. 12), and thus, likely no difference in the electrochemical oxidation mechanisms between the two anodes.

The rates of the non-electrochemical oxidation reactions (reaction (5) and reverse of reaction (6)) may be different on the two types of anodes and thereby influence carbon accumulation. Gas composition analysis done on electrolyte-supported cells with a Ni/YSZ anode and a $La_{0.3}Sr_{0.7}TiO_3$ conduction layer operated in dry CH_4 at 1023 K showed that for current densities less than 100 mA cm^{-2}, the main electrochemical products were CO and H_2O, whereas the CO_2 production was insignificant [41]. Hence for operating conditions used in the present study, the removal of carbon by CO_2 gasification (reverse of reaction (6)) may not be significant, and the lower amount of carbon accumulated on the Ni/YSZ than SnI–Ni/YSZ anodes could be due to the better carbon gasification by steam on the Ni/YSZ anodes (reaction (5)). In support of this argument, a previous study [5] on the gasification of carbon by steam has shown that Ni has higher gasification rates than 1% Sn-doped Ni. The product of gasification, CO, adsorbs more strongly on Sn-doped Ni than monometallic Ni [42] and may slow down the gasification rate. The segregation of Sn to the Ni surface may also reduce the number of Ni gasification sites, further slowing down the gasification rate and resulting in higher carbon accumulation on the SnI–Ni/YSZ anodes.

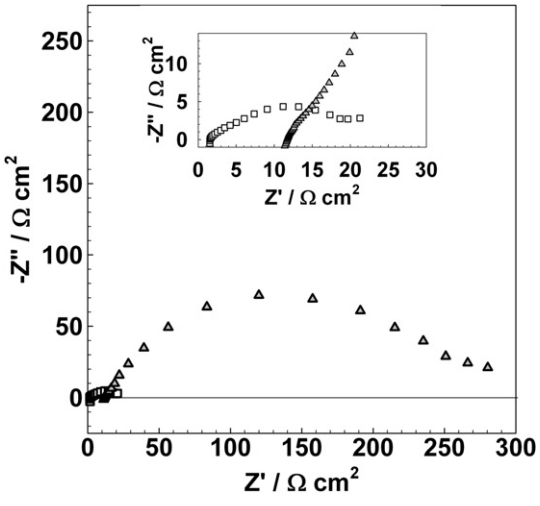

Fig. 9. Electrochemical impedance spectra of SOFC with 5% SnI–Ni/YSZ anode after exposure to dry CH_4 at OCV for 1 h (□) and 25 h (Δ) at 1073 K.

Previous reports [25–27] showed increased operational stability of SOFC with Sn-doped Ni/YSZ anodes. The improved operational stability was attributed to the better carbon tolerance of Sn-doped Ni/YSZ. In the studies [25–27], anode-supported SOFC (anode – 1000–1200 μm) were used, whereas electrolyte-supported SOFC (anode – 100 μm) were used in the present study. Comparison of results between anodes of different thicknesses is complex because a thicker anode provides more area for non-electrochemical reactions such as cracking and reforming of hydrocarbons [36]. So the composition of fuel that reaches the electrochemically active region is different for the anode- and electrolyte-supported cells [43]. In addition, the Sn may influence the microstructure, which strongly impacts performance. In our previous work [44], we showed that incorporation of Sn in the Ni/YSZ anode before the sintering stage of the fabrication process increased the shrinkage of the Ni/YSZ anodes by ~12% and this change in microstructure may also influence the operational stability.

Previous studies [5,28] involving steam reforming processes have shown that doping Ni with Sn reduces carbon formation. The comparison between supported Ni catalysts used for steam reforming and Ni/YSZ anode used in SOFC is not straightforward because of the difference in Ni particle size and amount. Supported Ni catalysts used in steam reforming have Ni contents of 15–20 wt% and are comprised of nano-sized Ni particles. Ni/YSZ anodes have more than 40 wt% Ni and micron-sized Ni and YSZ particles. The

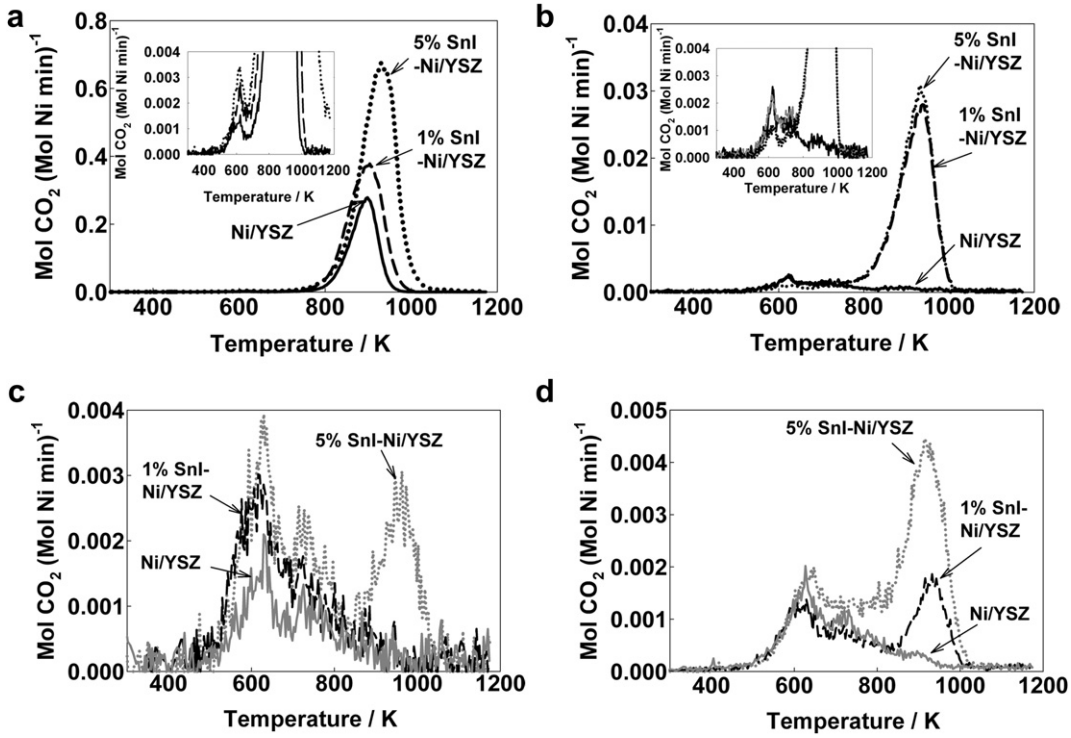

Fig. 10. CO_2 production during temperature programmed oxidation of Ni/YSZ (solid line), 1% SnI–Ni/YSZ (broken line) and 5% SnI–Ni/YSZ (dotted line) anodes after operation at 1073 K for 25 h in (a) dry CH_4 at OCV, (b) dry CH_4 at 10 mA cm^{-2}, (c) humidified CH_4 at 50 mA cm^{-2} and (d) after operation at 0.6 V and 1013 K in dry CH_4 for 25 h.

particle size of Ni is known to influence the carbon formation with smaller particles being more tolerant to carbon formation [29]. Also there are differences in the feed compositions between studies with steam to carbon ratios of 0.3 [5] and 1 [28], compared to the maximum ratio of 0.03 (for the cells operated in humidified CH_4) in the present study. Lay et al. [45] have also observed that addition of 1% Sn to Ni/YSZ anodes did not reduce carbon formation at such low steam to carbon ratios. Hence, the addition of Sn to Ni may not help improve the carbon tolerance of Ni/YSZ anodes operated at low steam to carbon ratios.

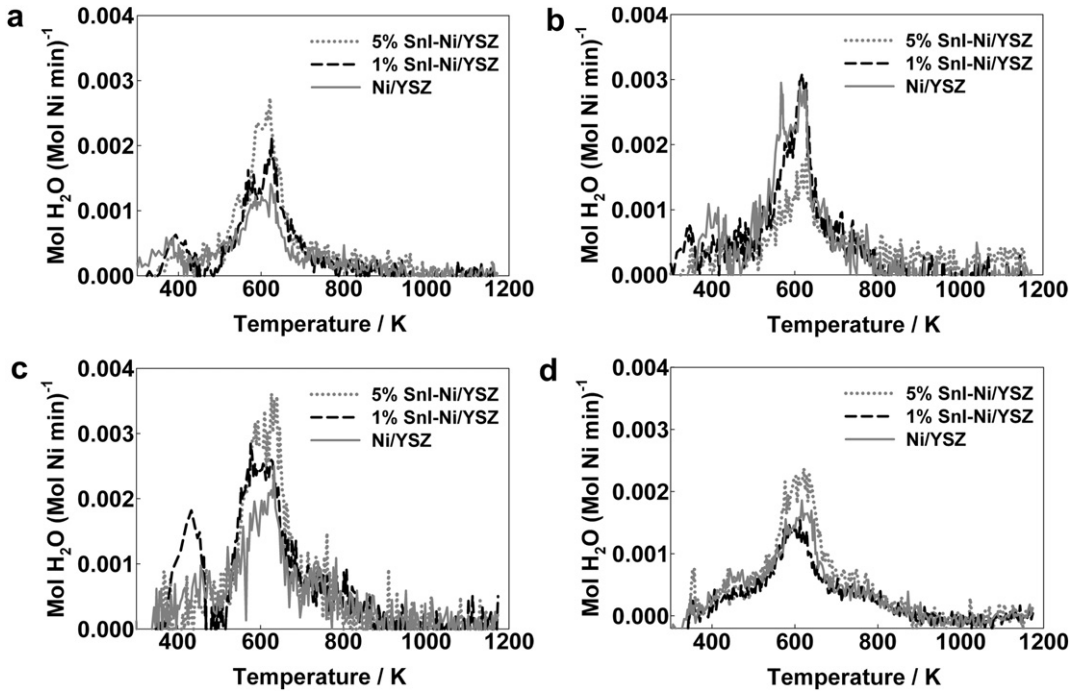

Fig. 11. H_2O production during temperature programmed oxidation of Ni/YSZ (solid line), 1% SnI–Ni/YSZ (broken line) and 5% SnI–Ni/YSZ (dotted line) anodes after operation at 1073 K for 25 h in (a) dry CH_4 at OCV, (b) dry CH_4 at 10 mA cm^{-2}, (c) humidified CH_4 at 50 mA cm^{-2} and (d) after operation at 0.6 V and 1013 K in dry CH_4 for 25 h.

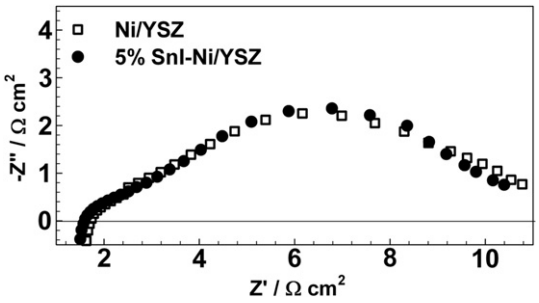

Fig. 12. Electrochemical impedance spectra done at 10 mA cm^{-2} with 1 mA amplitude on SOFC with Ni/YSZ (□) and 5% SnI–Ni/YSZ (●) anode after operation in dry CH_4 at 10 mA cm^{-2} and 1073 K for 25 h.

Nikolla et al. [25,28] proposed three mechanisms to explain the improvement in carbon tolerance of sn-doped Ni catalysts for steam reforming – Sn atoms displacing low-coordinated Ni atoms that act as carbon nucleation centers; Sn lowering the adsorption energy of carbon and CH_x fragments on the Ni surface, thereby reducing the concentration of carbon species on the Ni surface and reducing the driving force to form carbon deposits; and Sn increasing the barrier for C–C bond formation, while only slightly increasing the barrier for C–O bond formation. In the present study, the presence of Sn did not reduce carbon formation when SOFC were operated at low steam to carbon ratios (<0.03) and high temperatures. Also, the absence of a significant difference in adsorbed CH_x fragments (Type I carbon) on the Ni/YSZ and SnI–Ni/YSZ anodes (Figs. 10 and 11 and Table 2) suggests that there was no significant difference in the driving force to form carbon.

Similar to Sn, the carbon tolerance of additives like Au, S and K have been attributed to their preferential binding to the carbon nucleation sites of Ni [29]. However, there appears to be only a small temperature range in which these alloys have improved carbon tolerance relative to Ni/YSZ. This temperature range is 723–823 K for 1 wt% Sn–Ni/YSZ (see Fig. 3 in Ref. [28]) and 700–923 K for 6.4 wt% Au–Ni/YSZ (see Fig. 4b in Ref. [22]), when tested with dry CH_4. The results from the present study and other studies cited above show that additives like Sn and Au may not be stable at the carbon nucleation sites at high temperature and hence may not be able to influence the carbon nucleation and growth at these temperatures (1013 and 1073 K).

The influence of additives like K, Ca, Mn and Sn to Ni/Al_2O_3 on dry reforming of CH_4 and carbon formation was studied [46]. In the case of Ca, Mn and Sn, a dramatic reduction of catalytic activity and a significant increase in carbon deposition were observed after 30 h at 1023 K. The only additive that reduced the carbon formation was K. The carbon tolerance in the presence of K was attributed to the blockage of sites for methane cracking and to the good catalytic

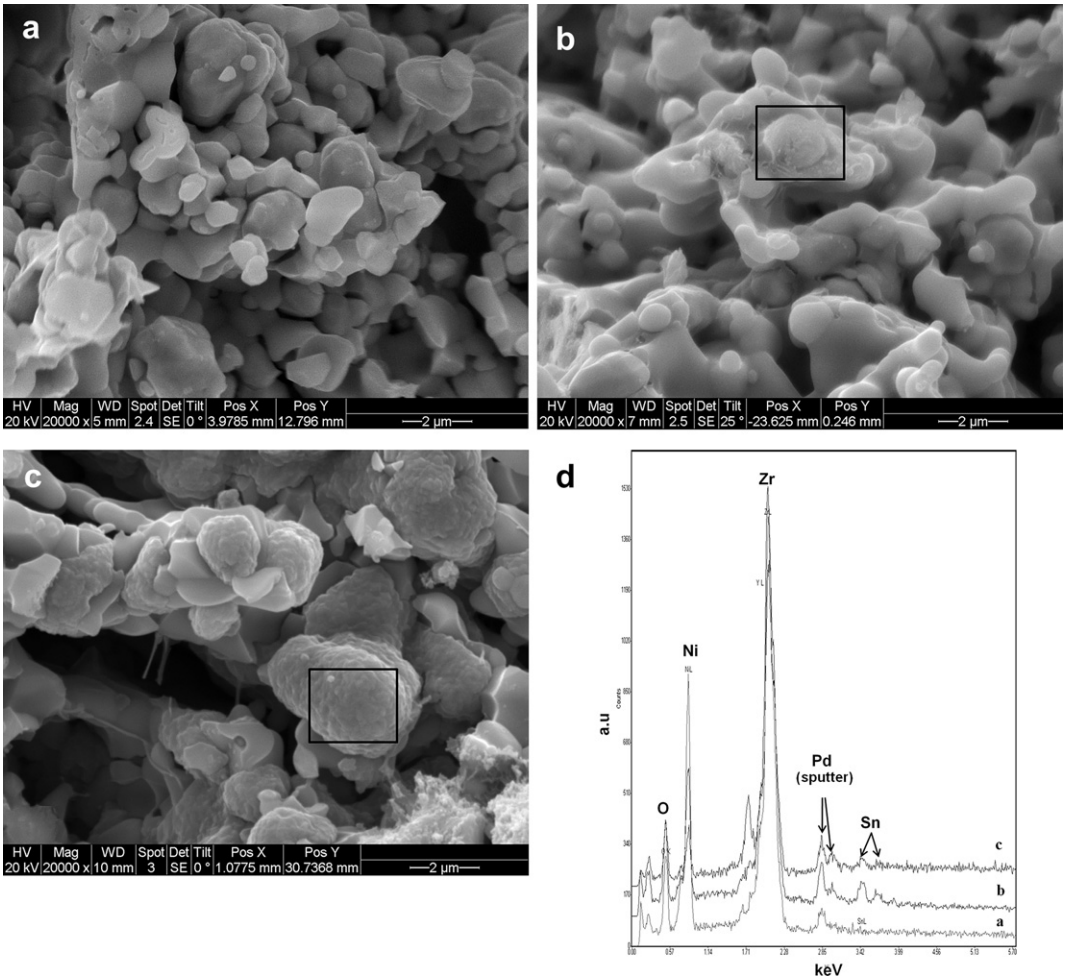

Fig. 13. SEM cross-sectional images of (a) Ni/YSZ and (b) 5% SnI–Ni/YSZ anode reduced in H_2 at 1073 K for 2 h, (c) 5% SnI–Ni/YSZ anode after testing in H_2 for 5 h followed by galvanostatic testing in dry CH_4 at 10 mA cm^{-2} and 1073 K for 25 h, (d) EDX spectra of the full region in (a) and the region inside the squares in (b) and (c).

activity of K for carbon gasification, which is consistent with our observation that gasification of carbon plays a significant role in determining the carbon tolerance of Ni/YSZ anodes.

The above discussion shows the importance of the carbon removal reactions in improving the carbon tolerance of the Ni/YSZ anodes. With this perspective, recent work on BaO addition to Ni looks promising [20]. BaO/Ni interfaces adsorb water and promote water-mediated carbon removal reactions [20]. Improving the carbon tolerance of Ni-based anodes by replacing YSZ with oxides like $CeZrO_2$ [47,48], which supply oxygen more efficiently to the Ni surface (spillover reaction) for carbon removal reactions, also may be a promising technique.

3.4. Sn stability

Sn content in 5% SnI–Ni/YSZ anodes were measured by EDX (Fig. 13) before and after electrochemical testing. The EDX analysis showed that the Sn/Ni wt. ratio decreased from 3.8 ± 0.4% to 2.2 ± 0.6% after electrochemical testing (5 h in H_2 followed by 25 h in CH_4 at 1073 K). A similar observation has been made by Kan et al. [27] for Sn-doped Ni/YSZ anodes after operation at 1073 K. The exact mechanism of the loss of Sn during operation at 1073 K is not clear and the identification of this mechanism is beyond the scope of this paper. However, the loss of Sn during operation at 1073 K indicates that under these conditions, it may be very difficult to retain the Sn in the anode for long durations (>40,000 h) expected in stack operations.

4. Conclusions

Sn-impregnated Ni/YSZ anodes were fabricated and their electrochemical performance, stability and carbon tolerance were compared to Ni/YSZ anodes. The electrochemical performance in H_2 and CH_4 decreased when the Sn content was increased from 1 to 5%. XPS analysis showed that Sn segregated to the surface of the Ni particle. This surface segregation may lead to Sn occupying the electrochemically active Ni sites thereby increasing the polarization resistance. The operational stability of Ni/YSZ anodes in CH_4 was not significantly influenced by the addition of Sn. The anode microstructure was also not altered or damaged by the addition of Sn by impregnation. The presence of Sn did not have a significant influence on the carbon formation on Ni/YSZ anodes. The higher amount of carbon accumulated on SnI–Ni/YSZ than Ni/YSZ anodes, however, indicated that the presence of Sn impeded the carbon removal reactions. Hence, at low steam to carbon ratios (<0.03) and temperatures (1013 K and 1073 K) used in this study, the addition of Sn did not improve the carbon tolerance of Ni/YSZ anodes operated in CH_4, and the Sn content in the anode decreased after operation at 1073 K for 30 h.

Acknowledgments

This work was supported through funding to the NSERC Solid Oxide Fuel Cell Canada Strategic Research Network from the Natural Science and Engineering Research Council (NSERC) and other sponsors listed in www.sofccanada.com. The authors also wish to thank Mr. M. A. Buccheri and Mr. S. Islam for useful discussions.

References

[1] S.C. Singhal, Solid State Ionics 152–153 (2002) 405–410.
[2] D.J.L. Brett, A. Atkinson, N.P. Brandon, S.J. Skinner, Chem. Soc. Rev. 37 (2008) 1568–1578.
[3] S. McIntosh, R.J. Gorte, Chem. Rev. 104 (2004) 4845–4865.
[4] A. Atkinson, S. Barnett, R.J. Gorte, J.T.S. Irvine, A.J. McEvoy, M. Mogensen, S.C. Singhal, J. Vohs, Nat. Mater. 3 (2004) 17–27.
[5] D.L. Trimm, Catal. Today 49 (1999) 3–10.
[6] H. He, J.M. Hill, Appl. Catal., A 317 (2007) 284–292.
[7] K. Ahmed, K. Foger, Catal. Today 63 (2000) 479–487.
[8] R. Craciun, S. Park, R.J. Gorte, J.M. Vohs, C. Wang, W.L. Worrell, J. Electrochem. Soc. 146 (1999) 4019–4022.
[9] M.D. Gross, J.M. Vohs, R.J. Gorte, J. Mater. Chem. 17 (2007) 3071–3077.
[10] S. Tao, J.T.S. Irvine, Nat. Mater. 2 (2003) 320–323.
[11] J.C. Ruiz-Morales, J. Canales-Vazquez, C. Savaniu, D. Marrero-Lopez, W. Zhou, J.T.S. Irvine, Nature 439 (2006) 568–571.
[12] Y.-H. Huang, R.I. Dass, Z.-L. Xing, J.B. Goodenough, Science 312 (2006) 254–257.
[13] S. Zha, P. Tsang, Z. Cheng, M. Liu, J. Solid State Chem. 178 (2005) 1844–1850.
[14] M.H. Pihlatie, A. Kaiser, M. Mogensen, M. Chen, Solid State Ionics 189 (2011) 82–90.
[15] F. Tietz, F.J. Dias, D. Simwonis, D. Stöver, J. Eur. Ceram. Soc. 20 (2000) 1023–1034.
[16] L. Yang, S. Wang, K. Blinn, M. Liu, Z. Liu, Z. Cheng, M. Liu, Science 326 (2009) 126–129.
[17] M. Mogensen, S. Primdahl, M.J. Jorgensen, C. Bagger, J. Electroceram. 5 (2000) 141–152.
[18] T. Takeguchi, Y. Kani, T. Yano, R. Kikuchi, K. Eguchi, K. Tsujimoto, Y. Uchida, A. Ueno, K. Omoshiki, M. Aizawa, J. Power Sources 112 (2002) 588–595.
[19] M. Asamoto, S. Miyake, K. Sugihara, H. Yahiro, Electrochem. Commun. 11 (2009) 1508–1511.
[20] L. Yang, Y. Choi, W. Qin, H. Chen, K. Blinn, M. Liu, P. Liu, J. Bai, T.A. Tyson, M. Liu, Nat. Commun. 2 (2011). doi:10.1038/ncomms1359 Article number: 357.
[21] T. Takeguchi, R. Kikuchi, T. Yano, K. Eguchi, K. Murata, Catal. Today 84 (2003) 217–222.
[22] I. Gavrielatos, V. Drakopoulos, S.G. Neophytides, J. Catal. 259 (2008) 75–84.
[23] N.C. Triantafyllopoulos, S.G. Neophytides, J. Catal. 239 (2006) 187–199.
[24] I. Gavrielatos, D. Montinaro, A. Orfanidi, S.G. Neophytides, Fuel Cells 9 (2009) 883–890.
[25] E. Nikolla, J. Schwank, S. Linic, J. Electrochem. Soc. 156 (2009) B1312–B1316.
[26] H. Kan, H. Lee, Appl. Catal., B 97 (2010) 108–114.
[27] H. Kan, S.H. Hyun, Y.-G. Shul, H. Lee, Catal. Commun. 11 (2009) 180–183.
[28] E. Nikolla, J. Schwank, S. Linic, J. Catal. 263 (2009) 220–227.
[29] H.S. Bengaard, J.K. Nørskov, J. Sehested, B.S. Clausen, L.P. Nielsen, A.M. Molenbroek, J.R. Rostrup-Nielsen, J. Catal. 209 (2002) 365–384.
[30] O.A. Marina, C.A. Coyle, M.H. Engelhard, L.R. Pederson, J. Electrochem. Soc. 158 (2011) B424–B429.
[31] B.C. Eigenbrodt, M.B. Pomfret, D.A. Steinhurst, J.C. Owrutsky, R.A. Walker, J. Phys. Chem. C 115 (2011) 2895–2903.
[32] D.J.L. Brett, A.R. Kucernak, P. Aguiar, S.C. Atkins, N.P. Brandon, R. Clague, L.F. Cohen, G. Hinds, C. Kalyvas, G.J. Offer, B. Ladewig, R. Maher, A. Marquis, P. Shearing, N. Vasileiadis, V. Vesovic, ChemPhysChem 11 (2010) 2714–2731.
[33] V. Alzate-Restrepo, J.M. Hill, Appl. Catal., A 342 (2008) 49–55.
[34] E.P. Murray, S.J. Harris, J. Liu, S.A. Barnett, Electrochem. Solid-State Lett. 9 (2006) A292–A294.
[35] J. Zhang, P. Munroe, D.J. Young, Acta Mater. 56 (2008) 68–77.
[36] M.A. Buccheri, A. Singh, J.M. Hill, J. Power Sources 196 (2011) 968–976.
[37] K. Nikooyeh, R. Clemmer, V. Alzate-Restrepo, J.M. Hill, Appl. Catal., A 347 (2008) 106–111.
[38] C.M. Finnerty, N.J. Coe, R.H. Cunningham, R.M. Ormerod, Catal. Today 46 (1998) 137–145.
[39] M. Yoshinaga, H. Kishimoto, K. Yamaji, Y.-P. Xiong, M.E. Brito, T. Horita, H. Yokokawa, Solid State Ionics 192 (2011) 571–575.
[40] M.B. Pomfret, J. Marda, G.S. Jackson, B.W. Eichhorn, A.M. Dean, R.A. Walker, J. Phys. Chem. C 112 (2008) 5232–5240.
[41] M.A. Buccheri, J.M. Hill, J. Electrochem. Soc. 159 (2012) B361–B367.
[42] R.L. Martins, M.A.S. Baldanza, A.L. Alberton, S.M.R. Vasconcelos, S.F. Moya, M. Schmal, Appl. Catal., B 103 (2011) 326–335.
[43] M. Cimenti, J.M. Hill, Energies 2 (2009) 377–410.
[44] A. Singh, J.M. Hill, ECS Trans. 35 (2011) 1397–1406.
[45] E. Lay, C. Metcalfe, O. Kesler, ECS Trans. 35 (2011) 1303–1313.
[46] A.E. Castro Luna, M.E. Iriarte, Appl. Catal., A 343 (2008) 10–15.
[47] M. Shishkin, T. Ziegler, ECS Trans. 35 (2011) 1611–1619.
[48] M. Cimenti, V. Alzate-Restrepo, J.M. Hill, J. Power Sources 195 (2010) 4002–4012.